

Multiple Stable Isoprene–Ozone Complexes Reveal Complex Entrance Channel Dynamics in the Isoprene + Ozone Reaction

Manoj Kumar, James Shee, Benjamin Rudshteyn, David R. Reichman, Richard A. Friesner, Charles E. Miller, and Joseph S. Francisco*



Cite This: *J. Am. Chem. Soc.* 2020, 142, 10806–10813



Read Online

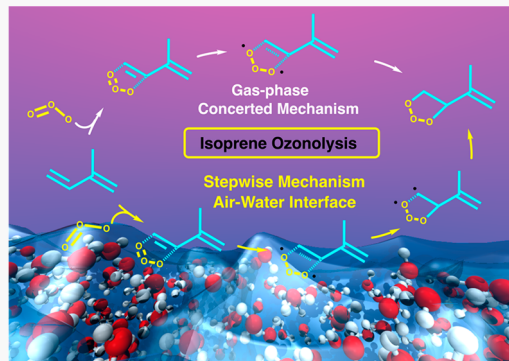
ACCESS |

Metrics & More

Article Recommendations

Supporting Information

ABSTRACT: Accurately characterizing isoprene ozonolysis continues to challenge atmospheric chemists. The reaction is believed to be a spontaneous, concerted cycloaddition. However, little information is available about the entrance channel and isoprene–ozone complexes thought to define the long-range portion of the reaction coordinate. Our coupled cluster and auxiliary field quantum Monte Carlo calculations predict multiple stable isoprene–ozone van der Waals complexes for *trans*-isoprene in the gas phase with moderate association energies. These results indicate that long-range dynamics in the isoprene–ozone entrance channel can impact the overall reaction in the troposphere and provide the spectroscopic information necessary to extend the microwave characterization of isoprene ozonolysis to prereactive complexes. At the air–water interface, Born–Oppenheimer molecular dynamics simulations indicate that the cycloaddition reaction between ozone and *trans*-isoprene follows a stepwise mechanism, which is quite distinct from our proposed gas-phase mechanism and occurs on a femtosecond time scale. The stepwise nature of isoprene ozonolysis on the aqueous surface is more consistent with the DeMore mechanism than with the Criegee mechanism suggested by the gas-phase calculations, suggesting that the reaction media may play an important role in the reaction. Overall, these predictions aim to provide a missing fundamental piece of molecular insight into isoprene ozonolysis, which has broad tropospheric implications due to its critical role as a nighttime source of hydroxyl radicals.



INTRODUCTION

Volatile organic compounds (VOCs) emitted from vegetation significantly impact atmospheric photochemistry. This biogenic carbon flux is dominated by isoprene or 2-methyl-1,3-butadiene (a conjugated diene with a chemical formula of C_5H_8). The emissions of isoprene are comparable to those of methane and make up nearly half of the total biogenic emissions of nonmethane VOCs worldwide.¹ Unlike methane, which has an atmospheric lifetime of nearly a decade, isoprene has a daytime half-life of less than 2 h and is rapidly oxidized by atmospheric oxidants such as the hydroxyl radical and ozone.^{2,3} Under typical atmospheric conditions, the reaction of isoprene with the OH radical is the dominant sink, followed by ozone (O_3), the nitrate radical, and the chlorine radical.^{4,5} Although the reaction with OH is the most dominant isoprene loss process, the ozone reaction accounts for nearly 10% of isoprene removal in the atmosphere.^{4,6}

The ozonolysis of isoprene in the atmosphere is an important reaction which has long been the subject of detailed chemical and physical characterization.⁷ The reaction is expected to be a spontaneous, concerted cycloaddition, proceeding via multiple ozonides and Criegee intermediates, and is a key source of the nonphotochemical hydroxyl radical,

which is a well-known oxidant in the troposphere.^{7–11} Besides that, the ozonolysis of isoprene serves as a source of organic peroxy radicals, a complex set of stable and radical products, and secondary organic aerosols (SOAs) in the atmosphere.^{7,12–14} Current observational studies have suggested that the isoprene-based SOA accounts for a significant fraction (~40%) of the total organic aerosols.^{15–17} A number of studies have reported the rate constants for the reactions of isoprene with ozone. The measured rate constants are generally in good agreement. For a comprehensive review of these rate constants, see ref 7. The IUPAC recommended rate constant for the isoprene–ozone reaction is described by $(1.03 \times 10^{-14})e^{(-1995 K/T)} \text{ cm}^3 \text{ molecule}^{-1} \text{ s}^{-1}$.⁴ There is extensive experimental work suggesting that the measured OH radical yield from the isoprene–ozone reaction is about 0.25. For example, Paulson et al.¹⁸ measured the OH radical formation

Received: February 28, 2020

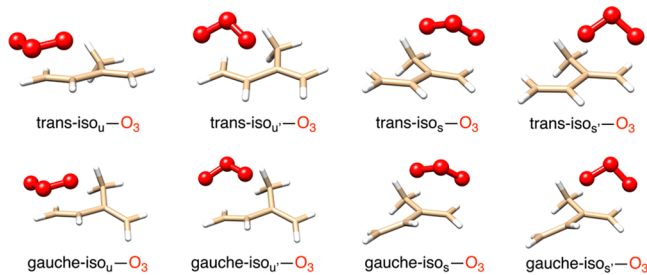
Published: May 20, 2020



from the reactions of ozone with isoprene, pinene, and methyl vinyl ketone. The measured OH yields were 0.25 ± 0.06 , 0.70 ± 0.17 , and 0.16 ± 0.05 for isoprene, pinene, and methyl vinyl ketone, respectively. A comprehensive review of the branching ratio results suggests that the steric hindrance of the CH_3 group outweighs its electron-donating effects, slightly favoring attack at $\text{C}3=\text{C}4$ (60% yield of the 3,4 primary ozonide) vs attack at $\text{C}1=\text{C}2$ (40% yield of the 1,2 primary ozonide).⁷ Recent results using short reaction times (~ 10 s) followed by product trapping in a 4 K buffer gas cell suggest that $\text{C}3=\text{C}4$ attack is favored 2:1 over $\text{C}1=\text{C}2$ attack.¹⁹

Despite extensive studies on the products of isoprene ozonolysis, there has been relatively little investigation of the entrance channel dynamics. The majority of what is known about the entrance channel for the ozone–isoprene reaction traces back to work on the ozone–ethene system.^{20–23} The ozone–ethene van der Waals complex has been observed by microwave spectroscopy.^{20,21} The structure of the van der Waals complex resembles the postulated transition-state structure,²⁰ strongly suggesting that it lies along the reaction coordinate for cycloaddition.²³ As a result, the structural results obtained from complex characterization provide detailed information about the geometry of the species at long distances along the reaction coordinate.²¹ The case of isoprene is complicated by the fact that there are two distinct double-bond sites that could potentially be involved in the reaction (Scheme 1).

Scheme 1. Different Stereochemical Possibilities for the Ozone Attack on *trans* and *gauche* Isoprene Double Bonds, Where *u* Represents Unsubstituted and *s* Represents Substituted, Based on the Proximity to the Methyl Group



As with the ozone–ethene complex,⁵ the ozone–isoprene complexes are thought to be precursors to the actual cycloaddition products,^{19,22} which means that the stereochemical properties of the reaction products are influenced by the stereochemistry of the complexes. Gillies et al.²⁴ employed *trans*- and *cis*-ethene-1-2-*d*₂ in an elegant stereochemical demonstration in which ethene ozonolysis is a concerted cycloaddition: the ozonolysis of *trans*-ethene-1-2-*d*₂ yielded exclusively *trans*-*d*₂ primary ozonides while the ozonolysis of *cis*-ethene-1-2-*d*₂ yielded equimolar mixtures of the *endo*- and *exo*-*d*₂ primary ozonides with no evidence for stereo randomization about the $\text{C}=\text{C}$ double bond.²³ Investigations of isoprene–ozone complexes must therefore consider the stereochemistry of the ozone attack on each double bond. However, technically because of the symmetry of isoprene, in principle, two pairs of products after addition are enantiomers and should have otherwise identical properties. Nonetheless, since we are interested in investigating the impact of the orientation of the central oxygen of ozone on the overall

reaction, we have considered all of the possibilities for the *trans*-isoprene–ozone reactions.

An additional complexity of the isoprene–ozone reaction is that isoprene has stable *trans* and *gauche* rotamers, as suggested by a previous study to be separated by ~ 2.4 kcal/mol.²⁵ There are, thus, two double-bond sites for each of two rotamers and two different stereochemical orientations of the ozone attack for a total of eight separate isoprene–ozone reaction coordinates and the potential for eight distinct isoprene–ozone van der Waals complexes (Scheme 1), where we investigate the approach from one face or one enantiomer.

Computational attempts have been made in the past to study the isoprene–ozone cycloaddition reaction. Zhang and Zhang²² studied the reaction using several theoretical methods. Interestingly, DFT calculations with the B3LYP functional and MP2 calculations suggested that the transition states for the cycloaddition reaction lie 1.6–2.3 and 4.8–6.1 kcal/mol below the separated reactants, respectively. However, the transition states predicted by CCSD(T) (affordable only in small basis sets such as 6-31G(d)) are found to lie 2.1–2.6 and 3.3–3.4 kcal/mol above the separated reactants, respectively. Kuwata and Valin²⁶ applied the CBS-QB3 method to estimate the cycloaddition barrier. However, this level of theory predicts the cycloaddition to be barrierless as the transition state is found to be 1.8–5.5 kcal/mol below the separated reactants. These results suggest that the B3LYP, MP2, and even CBS-QB3 methods are incapable of accurately describing the ozone reactions with reliable accuracy. This highlights the sensitivity of computational predictions to the choice of the density functional or the order of perturbation theory or coupled-cluster theory.

In this work, we use state of the art *ab initio* methods which can accurately model multireference electronic structure found in diradicals and stretched bond lengths to investigate the structure and energetics of these isoprene–ozone van der Waals complexes, yielding new insights regarding the possible reaction mechanism. In addition, we show that environmental effects at the air–water interface can significantly modulate the reaction mechanism.

COMPUTATIONAL METHODS

All gas-phase structures used in the present work were optimized with restricted DFT using the M06-2X functional²⁷ and the aug-cc-pVQZ^{28,29} basis set. We found that the use of unrestricted orbitals in the optimizations did not significantly affect the resulting geometries. Harmonic vibrational frequency analyses were performed to confirm the identity of stationary points and to estimate zero-point energies. We note that the energetic quantities presented in this work are the sum of electronic and zero-point energies and thus represent Gibbs free energies at zero temperature (though we acknowledge that typical tropospheric conditions range from -55 to 15 °C). Intrinsic reaction coordinate (IRC) calculations were performed to ensure that the transition states were connected to the appropriate prereaction complex and postreaction adduct, respectively. All gas-phase DFT calculations were performed with the Gaussian 09³⁰ quantum chemistry package.

The energetics of the various stationary points involved in the reactions were subsequently calculated by performing single-point calculations with DLPNO-CCSD(T), which is a localized version of the CCSD(T) method developed by Neese and co-workers that uses the semicanonical T_0 approximation.³¹ This method has been shown to recover 99.86% of the CCSD(T) correlation energy for a data set of organic molecules.^{32–34} Unrestricted Hartree–Fock reference wave functions, which, compared to the restricted orbital formalism, can

provide a more physical zeroth-order description of the electronic structure of ozone-involving chemistries and bond-forming processes, were utilized in all DLPNO-CCSD(T) calculations. The cc-pVTZ and cc-pVQZ basis sets were used to estimate the complete basis set (CBS) limit using the method built into the ORCA program.³⁵

We also calculated the energetics of stationary points using a stochastic electronic structure method, phaseless auxiliary-field quantum Monte Carlo (ph-AFQMC), that samples ground-state observables via solving the imaginary-time Schrödinger equation.^{36,37} This approach has recently been shown to achieve very high accuracy for a variety of strongly correlated molecules, including organic diradicals, polyacenes,³⁸ and transition-metal-containing systems,³⁹ and, notably, is capable of doing so even when CCSD(T) methods break down. Given the nontrivial diradical electronic structure involved in the ozone molecule^{32–34,40–42} and, in general, the multireference character exhibited when bonds are stretched beyond equilibrium lengths, we utilize ph-AFQMC as a reliable methodology for studying isoprene–ozone chemistries. We perform ph-AFQMC calculations with multideterminant trial wave functions in the cc-pVTZ basis and compute the CBS correction from scaled DLPNO-CCSD(T) calculations in the cc-pVTZ and cc-pVQZ basis sets.⁴³ The statistical uncertainties in absolute energies represent the standard errors in energy measurements sampled along imaginary-time trajectories. The reported statistical error bars for energy differences are then obtained by quadrature. Further methodological details can be found in the SI.

Born–Oppenheimer molecular dynamics (BOMD) simulations were performed on the basis of potentials derived from unrestricted DFT, specifically the Becke–Lee–Yang–Parr (BLYP)^{44,45} functional with Grimme's dispersion correction (D3)^{46,47} as implemented in the CP2K⁴⁸ code. The droplet system contained 191 water molecules, 1 *trans*-isoprene molecule, and 1 ozone molecule. The water droplet was used as a simplistic representation of aerosol particles, clouds, and aqueous surfaces prevalent in the troposphere.^{49–51} The configuration of the water droplet was first obtained by performing classical MD simulations for 5 ns with the COMPASS force field, followed by 5 ps (ps) BOMD simulations. The dimensions of the simulation box were $x = 35 \text{ \AA}$, $y = 35 \text{ \AA}$, and $z = 35 \text{ \AA}$, making the box large enough to avoid interactions between adjacent periodic images of the water droplet. Prior to the BOMD simulations, the system was fully relaxed using DFT with BLYP-D3. The selection of BLYP-D3 for studying isoprene–ozone chemistry at the air–water interface was driven by the ability of BLYP-D3 to accurately describe several bimolecular Criegee chemistries at the air–water interface.⁵¹ Since the Criegee intermediate and ozone have very similar electronic structures, the choice of the BLYP-D3 functional is reasonable for the present simulations. These BOMD simulations were performed with the unrestricted formalism (UBLYP-D3), which provides a better description of biradical chemistries. We note that while the gas-phase potential energy surface (Figure S4) shows slight differences to that calculated with the higher-level methods, the relatively low computational cost of BLYP-D3 enabled our BOMD simulations which yield essential information about the effects of the tropospheric environment on isoprene–ozone chemistry.

A double- ζ Gaussian basis set combined with an auxiliary basis set and Goedecker–Teter–Hutter (GTH) norm-conserved pseudopotentials was adopted to treat the valence electrons and core electrons, respectively.^{52,53} An energy cutoff of 280 Ry was set for the plane-wave basis set, and a cutoff of 40 Ry was set for the Gaussian basis set. The BOMD simulations were carried out in the constant volume and temperature (NVT) ensemble using the Nose–Hoover chain method to control the temperature (300 K) of the system. The integration step was set as 1 fs, which has been proven to achieve sufficient energy conservation in water systems.⁵¹

RESULTS

Isoprene–Ozone van der Waals Complexes. As a first step, we explored the conformational isomerization between the *trans* and *gauche* conformers of isoprene. Relevant states on

the potential energy surface, calculated at two different levels of theory, are displayed in Figure S1 (omitting the *gauche–gauche* transition state that is lower in energy than the *trans–gauche* transition state²⁵).

The *gauche* conformer with DLPNO-CCSD(T) is 2.8 kcal/mol less stable than the *trans* one, which is consistent with the previous, recent prediction of Frank and Doublerly using CCSD(T)-optimized structures with an ANO basis set.²⁵ The barrier height results are also similar as we discuss in the SI. ph-AFQMC calculations also predict the *gauche* conformer to be less stable by 3.2 ± 0.5 kcal/mol, which, given the statistical error bars, agrees with the DLPNO-CCSD(T) result.

Given that our calculations suggest that *trans*-isoprene is more stable than *gauche*-isoprene, we proceed now to explore the interaction of *trans*-isoprene with ozone. Ozone can interact with two double bonds in isoprene in four different ways (Scheme 1). We have represented the four complexes as *trans*-iso_u···O₃, *trans*-iso_{u'}···O₃, *trans*-iso_s···O₃, and *trans*-iso_{s'}···O₃. Here, u and s represent the unsubstituted and substituted double bonds in isoprene. The u'- and s'-containing complexes have a different orientation of central oxygen in O₃ compared to that of u- and s-containing complexes.

The M06-2X/aug-cc-pVDZ optimized geometries of these complexes along with their DLPNO-CCSD(T) and ph-AFQMC calculated binding energies are shown in Figure 1.

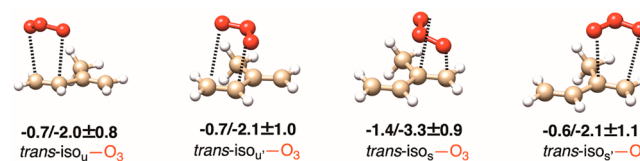


Figure 1. M06-2X/aug-cc-pVDZ optimized geometries of various *trans*-isoprene–ozone van der Waals complexes. The DLPNO-CCSD(T) and ph-AFQMC calculated binding energies of isoprene–O₃ complexes are shown to the left of and to the right of the “/”, respectively. All quantities are in kcal/mol units. The statistical error bars corresponding to the ph-AFQMC values are given in parentheses.

The DLPNO-CCSD(T) calculated binding energies of the *trans*-isoprene···O₃ association complexes are in the range of 0.6–1.4 kcal/mol. Interestingly, when restricted Hartree–Fock reference wave functions are utilized in the DLPNO-CCSD(T) calculations, the binding energies are increased to 1.1–1.6 kcal/mol, as shown in Figure S2. The binding energies computed with ph-AFQMC are noticeably larger in magnitude than those computed with DLPNO-CCSD(T), which is likely due to the relatively more accurate descriptions of ozone and elongated bond lengths provided by ph-AFQMC. Irrespective of the theoretical methodology used, the *trans*-iso_s···O₃ complex is predicted to be the most stable, with a binding energy of 1.4 kcal/mol via DLPNO-CCSD(T) which increased to 3.3 ± 0.9 kcal/mol when calculated with ph-AFQMC. The isoprene–O₃ association complexes are all true minima, which is indicative of association energies en route to the formation of their corresponding primary ozonides (POZs). This aspect of isoprene–O₃ chemistry has been underappreciated in previous studies.²²

Isoprene–Ozone Cycloaddition Reactions. The existence of stable *trans*-isoprene–O₃ complexes motivated us to establish the energetics of the corresponding cycloaddition reactions, which led to the formation of POZs. The detailed

reaction mechanisms of these *trans*-isoprene + O₃ → POZs reactions are illustrated in **Scheme 1**, whereas the calculated reaction profiles are shown in **Figure 2**. In **Figure S2**, we show the reaction profiles calculated with restricted DLPNO-CCSD(T) and the values obtained from ph-AFQMC when these restricted values are used in the basis set extrapolation.

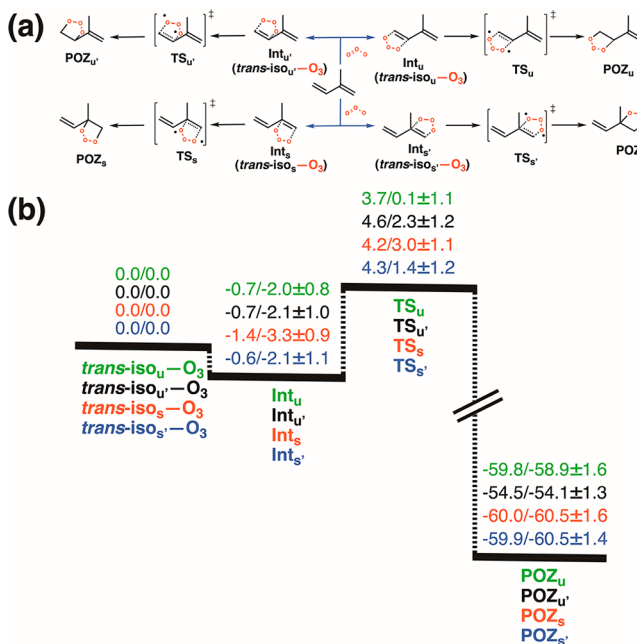


Figure 2. (a) Various primary ozonide (POZ)-forming reactions originating from the interaction of *trans*-isoprene with ozone. (b) The DLPNO-CCSD(T) and ph-AFQMC calculated reaction profiles, in kcal/mol units, for the primary ozonide-forming interaction of *trans*-isoprene with ozone. All energies are referenced relative to the energy of the separated reactants (0.0 kcal/mol). The DLPNO-CCSD(T) and ph-AFQMC predictions are shown to the left of and to the right of the “/”, respectively. The statistical error bars corresponding to the ph-AFQMC values are given. Here, Int notation is used to represent van der Waals *trans*-isoprene–O₃ complexes, whereas TS and POZ are used to represent corresponding transition states and primary ozonides.

The calculated rotational constants and harmonic vibrational frequencies of all stationary points involved in these cycloaddition reactions are given in **Tables S4–S8**. The optimized geometries of all structures reported here are given in **Tables S9–S13**. The calculations indicate a concerted reaction mechanism, and that, contrary to the previous assumption, the *trans*-isoprene–O₃ cycloaddition does occur via a pre-reaction minimum and confirms that the reaction has an appreciable barrier height, defined as the difference between the association complexes and the corresponding transition states. A range of 4.4–5.6 kcal/mol is calculated with DLPNO-CCSD(T), while values between 2.1 ± 1.4 and 6.3 ± 1.5 kcal/mol are calculated with ph-AFQMC. The energetics resulting from DFT calculations with the M06-2X functional, which was used in the geometry optimizations, are shown in **Figure S3**. Similar association and reaction energies were found, but with higher barriers. On the whole, this functional yields much more physical results compared to the MP2 and B3LYP methods used in ref 22.

The differing barrier heights predicted for the POZ-forming reactions originating from the *trans*-iso_u··O₃ and *trans*-iso_s··O₃

complexes are mainly due to the stereochemical environment for the olefinic attack of ozone in *trans*-isoprene in these conformers. Overall, the *trans*-isoprene–O₃ cycloaddition reactions are strongly exothermic in nature, with a reaction energy of between 54.5 and 60.5 kcal/mol. The calculated exothermicities for the POZ-forming reactions are consistent between both methods.

Thus, the presence of the van der Waals wells in the entrance channel has implications for the kinetics in the low-temperature region, suggesting that the complexes might have longer lifetimes than originally assumed. The experimental implications are twofold. First, the kinetics should show non-Arrhenius behavior in the low-temperature region. Second, if the complexes are sufficiently long-lived, they could dictate subsequent reactions involving the prereactive complex. This has not been discussed for isoprene–ozone chemistry before. We note, however, that future studies which account for the effect of the back-dissociation pathway are needed to make rigorous claims about reaction rates.

Isoprene–Ozone Cycloaddition Reaction at the Air–Water Interface. Because the gas-phase predictions suggest a viable cycloaddition reaction between *trans*-isoprene and ozone under tropospheric conditions, we next decided to explore whether the same reaction could also occur in heterogeneous environments prevalent in the troposphere. These heterogeneous environments include aqueous surfaces such as air–water or air–ice interfaces and wet material surfaces such as wet silica. We performed BOMD simulations to investigate the *trans*-isoprene–ozone cycloaddition originating from the *trans*-iso_u··O₃ complex at an air–water interface, which is a simplistic representation of aerosol surfaces, clouds, and the aqueous surfaces present in the troposphere.^{49–51} The selection of the *trans*-iso_u··O₃ complex was inspired by the fact that the gas-phase calculations predict the cycloaddition reaction between *trans*-isoprene and ozone from this complex to involve the lowest barrier at both levels of theory (**Figure 2**). Interestingly, the BOMD simulation results predict a cycloaddition mechanism at the air–water interface, which is different from that in the gas phase, i.e., the cycloaddition reaction at the air–water interface follows a stepwise mechanism (**Figure 3** and **Movie S1**) whereas the gas-phase reaction follows a concerted mechanism (**Figure 2**). The ability of the interfacial aqueous environment to stabilize charged intermediates probably accounts for the stepwise reaction. The interfacial cycloaddition reaction occurs over a femtosecond time scale, which is much faster than that predicted above in the gas phase and also quite interesting considering that the Criegee intermediate, which is generated following similar cycloadditions, has been found to react on a picosecond time scale.⁵¹

Interfacial cycloaddition is mediated by a prereaction complex (Int₁) at 0 fs (**Figure 3**). At this point, there is an interaction between O₃ and *trans*-isoprene, which is indicated by two key bond distances of C3–O1 = 2.53 Å and C4–O3 = 2.43 Å, whereas both the double bonds (C1=C2 = 1.35 Å and C3=C4 = 1.37 Å) in *trans*-isoprene are intact so far. At 97 fs, the transition-state-like structure (TS₁) for C4–O3 bond formation is formed in which the C4–O3 bond is 1.52 Å whereas the C3–O1 bond is 1.93 Å long. The C3=C4 bond has noticeably lengthened to 1.49 Å. The other double bond (C1=C2) remains unchanged throughout this cycloaddition reaction. This transient complex then transforms into the intermediate, Int₂ at 106 fs, in which the C4–O3 bond is fully

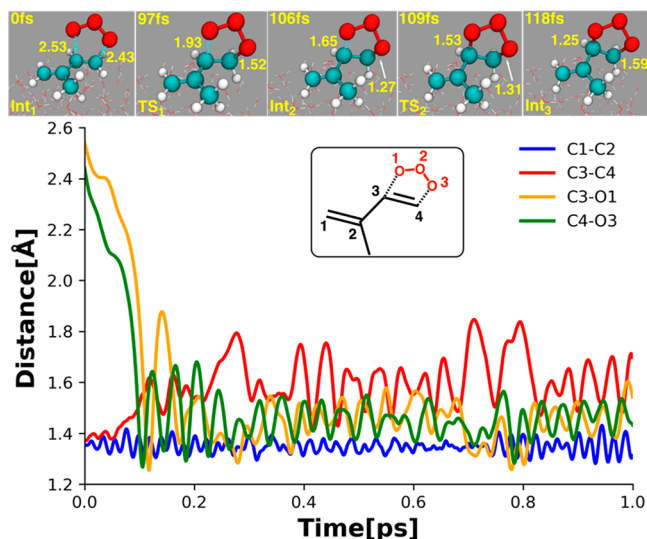


Figure 3. (Upper panel) Snapshot structures taken from the BOMD simulations, illustrating the stepwise cycloaddition of ozone across the C3=C4 double bond of *trans*-isoprene on a water droplet of 191 water molecules. (Lower panel) Time evolution of key bond distances involved in the multistep interfacial cycloaddition of ozone to *trans*-isoprene. The inset in the lower panel describes the atom numbering used in the discussion of BOMD simulation results.

formed (1.27 Å), which is also followed by a noticeable elongation of the C3–C4 bond to 1.55 Å. The C3–O1 bond at this stage is 1.65 Å. However, **Int**₂ remains stable only for a few femtoseconds as the transition-state-like structure for the C3–O1 bond formation (**TS**₂) is formed at 109 fs. The C3–O1 bond is now 1.53 Å, whereas the C4–O3 bond is 1.31 Å long. The C3–C4 bond is 1.56 Å. At 118 fs, the formation of POZ (**Int**₃) is complete, which is reflected in the C3–O1 and C4–O3 bond distances. Beyond that, the cycloadduct or POZ is found to remain stable despite the fact that the C3–O1 and C4–O3 bonds fluctuate for a few femtoseconds. Since the interfacial ozonolysis reaction is rapidly observed in the BOMD simulations, we have not simulated the reaction beyond 1500 fs. Over the simulated time scale, the oxygens of the POZ remain projected away from the water surface. Interestingly, an interfacial water molecule starts interacting with the double bond of the mono-ozonized isoprene via hydrogen bonding. This hydrogen bond is 2.60 Å long and has a bond angle of 164°. A snapshot is shown in Figure 4 in which there is close interaction between the carbons of the double bond and one of the interfacial water molecules. Specifically, the C1–H_w and C2–H_w bond lengths are 2.51 and 2.77 Å long at 1500 fs, respectively. The C1–H_w–O_w and C2–H_w–O_w bond angles are 177.7 and 151.2°, respectively. Overall, these BOMD simulation results provide the first definitive evidence of establishing the time scale of the ozone cycloaddition across an olefinic bond that has broad tropospheric implications.

According to Criegee,⁵⁴ the addition of ozone to an alkene proceeds via the 1,3-cycloaddition mechanism through the symmetric transition state to form a five-membered POZ in the first elementary step of the Criegee mechanism. This reaction mechanism was confirmed by several experimental studies.^{55–57} An alternative reaction mechanism, where ozone reacts with the double bond similarly to the peroxy radical to form the biradical transition state, was proposed by DeMore⁵⁸ and is usually referred to as the stepwise or DeMore

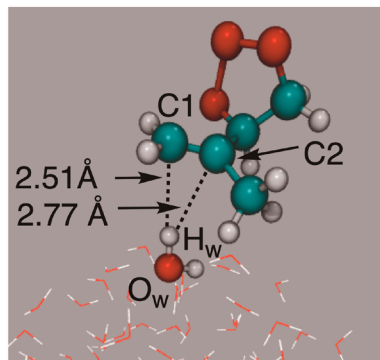


Figure 4. Snapshot structure taken from the BOMD simulations, illustrating the hydrogen bonding interaction between the C1=C2 double bond of *trans*-isoprene on a water droplet of 191 water molecules and an interfacial water molecule.

mechanism. Initially, this mechanism was suggested to be favored in the case of the ethyne reaction.⁵⁸ However, certain features of ozonolysis via the Criegee mechanism⁵⁹ indicate that the Criegee and DeMore mechanisms can compete efficiently, as influenced by the presence of substituents around the olefinic bond. It is proposed that the Criegee mechanism predominates in the case of the reaction of ozone with ethene^{59,60} and other studied alkenes, whereas the DeMore mechanism is preferred for tetrafluoroethene.⁶¹ Our gas-phase calculations, which suggest a concerted ozone addition across isoprene double bonds, are consistent with the Criegee mechanism. However, the BOMD simulations suggest that the ozone addition across an isoprenic double bond at the air–water interface occurs in a stepwise manner, which is more consistent with the DeMore-type addition mechanism. These results indicate that the reaction environment, in addition to substituent effects, is likely to play a crucial role in switching the ozonolysis mechanism from Criegee to DeMore type.

It is important to mention here that the reaction of isoprene and methacrolein with ozone has been previously investigated at different stages in the condensed phase at temperatures from 15 to 265 K by IR spectroscopy.⁶² It is thus interesting to compare our present simulation results with those previous findings. Ozone was preferentially cycloadded to the double bond of isoprene which is not methyl-substituted. The same preferential cycloaddition of ozone at the air–water interface is observed in the present simulations. However, while the ozonolysis of isoprene in that work followed a typical Criegee mechanism, our simulations predict a stepwise mechanism for the interfacial reaction, which is more consistent with the DeMore-type mechanism.

CONCLUSIONS

Our calculations suggest the existence of multiple stable isoprene–ozone complexes, which is indicative of complex entrance channel dynamics in the isoprene ozonolysis reaction. The calculations further suggest that the gas-phase reaction between *trans*-isoprene and ozone follows a concerted mechanism and involves moderate barrier heights, which should be accessible under tropospheric conditions. The BOMD simulations suggest that at the air–water interface the cycloaddition of ozone across the olefinic bond of isoprene follows a distinct stepwise mechanism and occurs on a femtosecond time scale. This is the first time the time scale of the olefin–ozone interaction has been established. The

stepwise nature of the isoprene ozonolysis is more consistent with the DeMore mechanism, suggesting that the reaction environment plays an important role in modulating the ozonolysis mechanism from Criegee to DeMore type. The present results reveal new molecular insights into a missing fundamental piece of isoprene ozonolysis chemistry, which has important tropospheric implications because of its role in the production of hydroxyl and peroxy radicals and secondary organic aerosols. In the upper troposphere, where the calculated well depths of the isoprene–ozone van der Waals complexes are greater than the available thermal energy, our results suggest that the prereactive complexes could be long-lived and thus detectable in molecular beam studies of the reaction with buffer gas cooling.

■ ASSOCIATED CONTENT

Supporting Information

The Supporting Information is available free of charge at <https://pubs.acs.org/doi/10.1021/jacs.0c02360>.

Details about the DLPNO-CCSD(T) and ph-AFQMC, results with the BLYP-D3 and M06-2X functionals, tables containing rotational constants and harmonic vibrational frequencies, and optimized geometries of various species examined in the present work (PDF)

Trajectories of the BOMD simulation for the *trans*-isoprene–ozone reaction at the air–water interface (MPG)

■ AUTHOR INFORMATION

Corresponding Author

Joseph S. Francisco — Department of Chemistry, University of Pennsylvania, Philadelphia, Pennsylvania 19104, United States;  orcid.org/0000-0002-5461-1486; Email: frjoseph@sas.upenn.edu

Authors

Manoj Kumar — Department of Chemistry, University of Pennsylvania, Philadelphia, Pennsylvania 19104, United States

James Shee — Department of Chemistry, Columbia University, New York, New York 10027, United States;  orcid.org/0000-0001-8333-8151

Benjamin Rudshteyn — Department of Chemistry, Columbia University, New York, New York 10027, United States;  orcid.org/0000-0002-9511-6780

David R. Reichman — Department of Chemistry, Columbia University, New York, New York 10027, United States

Richard A. Friesner — Department of Chemistry, Columbia University, New York, New York 10027, United States

Charles E. Miller — Jet Propulsion Laboratory, California Institute of Technology, Pasadena, California 91109, United States

Complete contact information is available at:

<https://pubs.acs.org/10.1021/jacs.0c02360>

Funding

D.R.R. acknowledges funding from NSF CHE-1464802. B.R. acknowledges funding from the National Institute of General Medical Sciences of the National Institutes of Health under award number F32GM136105.

Notes

The authors declare no competing financial interest.

■ ACKNOWLEDGMENTS

M.K. and J.S.F. acknowledge computing support from the Holland Computing Center, University of Nebraska—Lincoln for the Gaussian and CP2K calculations. This research used resources of the Oak Ridge Leadership Computing Facility at the Oak Ridge National Laboratory, which is supported by the Office of Science of the U.S. Department of Energy under contract no. DE-AC05-00OR22725. We thank Prof. Marsha Lester for her helpful comments on the manuscript.

■ REFERENCES

- (1) Guenther, A.; Jiang, X.; Heald, C. L.; Sakulyanontvittaya, T.; Duhl, T.; Emmons, L. K.; Wang, X. The model of emissions of gases and aerosols from nature version 2.1 (MEGAN 2.1): An extended and updated framework for modeling biogenic emissions. *Geosci. Model Dev.* **2012**, *5*, 1471–1492.
- (2) Chameides, W. L.; Fehsenfeld, F.; Rodgers, M. O.; Cardelino, C.; Martinez, J.; Parrish, D.; Lonneman, W.; Lawson, D. R.; Rasmussen, R. A.; Zimmerman, P.; Greenberg, J. Ozone precursor relationships in the ambient atmosphere. *J. Geophys. Res.* **1992**, *97*, 6037–6055.
- (3) Stone, D.; Evans, M. J.; Edwards, P. M.; Commane, R.; Ingham, T.; Rickard, A. R.; Brookes, D. M.; Hopkins, J.; Leigh, R. J.; Lewis, A. C.; Monks, P. S. Isoprene oxidation mechanisms: measurements and modelling of OH and HO₂ over a south-east Asian tropical rainforest during the OP₃ field campaign. *Atmos. Chem. Phys.* **2011**, *11*, 6749–6771.
- (4) Atkinson, R.; Baulch, D. L.; Cox, R. A.; Crowley, J. N.; Hampson, R. F.; Hynes, R. G.; Jenkin, M. E.; Rossi, M. J.; Troe, J. Evaluated kinetic and photochemical data for atmospheric chemistry: Volume 2: reactions of organic species. *Atmos. Chem. Phys.* **2006**, *6*, 3625–4055.
- (5) Burkholder, J. B.; Sander, S. P.; Abbatt, J.; Barker, J. R.; Huie, R. E.; Kolb, C. E.; Kurylo, M. J.; Orkin, V. L.; Wilmouth, D. M.; Wine, P. H. *Chemical Kinetics and Photochemical Data for Use in Atmospheric Studies*, evaluation no. 18; JPL publication 15-10; Jet Propulsion Laboratory: 2015.
- (6) Isidorov, V. A. *Organic Chemistry of the Earth's Atmosphere*; Springer-Verlag: 1990.
- (7) Wennberg, P. O.; Bates, K. H.; Crounse, J. D.; Dodson, L. G.; McVay, R. C.; Mertens, L. A.; Nguyen, T. B.; Praske, E.; Schwantes, R. H.; Smarte, M. D.; St. Clair, J. M.; Teng, A. P.; Zhang, X.; Seinfeld, J. H. Gas-phase reactions of isoprene and its major oxidation products. *Chem. Rev.* **2018**, *118*, 3337–3390.
- (8) Zhang, D.; Lei, W.; Zhang, R. Mechanism of OH formation from ozonolysis of isoprene: kinetics and product yields. *Chem. Phys. Lett.* **2002**, *358*, 171–179.
- (9) Paulson, S. E.; Orlando, J. J. The reactions of ozone with alkenes: An important source of HO_x in the boundary layer. *Geophys. Res. Lett.* **1996**, *23*, 3727–3730.
- (10) Kroll, J. H.; Hanisco, T. F.; Donahue, N. M.; Demerjian, K. L.; Anderson, J. G. Accurate, direct measurements of OH yields from gas-phase ozone-alkene reactions using an *in situ* LIF Instrument. *Geophys. Res. Lett.* **2001**, *28*, 3863.
- (11) Anglada, J. M.; Bofill, J. M.; Olivella, S.; Solé, A. Unimolecular isomerizations and oxygen atom loss in formaldehyde and acetaldehyde carbonyl oxides. A Theoretical Investigation. *J. Am. Chem. Soc.* **1996**, *118*, 4636–4647.
- (12) Kamens, R. M.; Gery, M. W.; Jeffries, H. E.; Jackson, M.; Cole, E. I. Ozone-isoprene reactions: Product formation and aerosol potential. *Int. J. Chem. Kinet.* **1982**, *14*, 955–975.
- (13) Biesenthal, T. A.; Bottenheim, J. W.; Shepson, P. B.; Li, S.-M.; Brickell, P. C. The chemistry of biogenic hydrocarbons at a rural site in eastern Canada. *J. Geophys. Res. - Atmos.* **1998**, *103*, 25487–25498.
- (14) Nguyen, T. B.; Bateman, A. P.; Bones, D. L.; Nizkorodov, S. A.; Laskin, J.; Laskin, A. High-resolution mass spectrometry analysis of

secondary organic aerosol generated by ozonolysis of isoprene. *Atmos. Environ.* **2010**, *44*, 1032–1042.

(15) Miyazaki, Y.; Fu, P. Q.; Kawamura, K.; Mizoguchi, Y.; Yamanoi, K. Seasonal variations of stable carbon isotopic composition and biogenic tracer compounds of water-soluble organic aerosols in a deciduous forest. *Atmos. Chem. Phys.* **2012**, *12*, 1367–1376.

(16) Fu, P.; Kawamura, K.; Chen, J.; Miyazaki, Y. Secondary Production of Organic Aerosols from Biogenic VOCs over Mt. Fuji, Japan. *Environ. Sci. Technol.* **2014**, *48*, 8491–8497.

(17) Nakayama, T.; Sato, K.; Imamura, T.; Matsumi, Y. Effect of oxidation process on complex refractive index of secondary organic aerosol generated from isoprene. *Environ. Sci. Technol.* **2018**, *52*, 2566–2574.

(18) Paulson, S. E.; Chung, M.; Sen, A. D.; Orzechowska, G. Measurement of OH radical formation from the reaction of ozone with several biogenic alkenes. *J. Geophys. Res. Lett.* **1998**, *103*, 25533–25539.

(19) Porterfield, J. P.; Eibenberger, S.; Patterson, D.; McCarthy, M. C. The ozonolysis of isoprene in a cryogenic buffer gas cell by high resolution microwave spectroscopy. *Phys. Chem. Chem. Phys.* **2018**, *20*, 16828–16834.

(20) Gillies, J. Z.; Gillies, C. W.; Suenram, R. D.; Lovas, F. J.; Stahl, W. The microwave spectrum and molecular structure of the ethylene–ozone van der Waals complex. *J. Am. Chem. Soc.* **1989**, *111*, 3073–3074.

(21) Gillies, C. W.; Gillies, J. Z.; Suenram, R. D.; Lovas, F. J.; Kraka, E.; Cremer, D. Van der Waals complexes in 1,3-dipolar cycloaddition reactions: ozone–ethylene. *J. Am. Chem. Soc.* **1991**, *113*, 2412–2421.

(22) Zhang, D.; Zhang, R. Mechanism of OH formation from ozonolysis of isoprene: A quantum-chemical study. *J. Am. Chem. Soc.* **2002**, *124*, 2692–2703.

(23) Kuczkowski, R. L. The structure and mechanism of formation of ozonides. *Chem. Soc. Rev.* **1992**, *21*, 79–83.

(24) Gillies, J. Z.; Gillies, C. W.; Suenram, R. D.; Lovas, F. J. The ozonolysis of ethylene: microwave Spectrum, molecular structure, and dipole moment of ethylene primary ozonide (1,2,3-trioxolane). *J. Am. Chem. Soc.* **1988**, *110*, 7991–7999.

(25) Franke, P. R.; Doublerly, G. E. Rotamers of isoprene: infrared spectroscopy in Helium droplets and *ab initio* thermochemistry. *J. Phys. Chem. A* **2018**, *122*, 148–158.

(26) Kuwata, K. T.; Valin, L. C. Quantum chemical and RRKM/master equation studies of isoprene ozonolysis: Methacrolein and methacrolein oxide. *Chem. Phys. Lett.* **2008**, *451*, 186–191.

(27) Zhao, Y.; Truhlar, D. G. The M06 suite of density functionals for main group thermochemistry, thermochemical kinetics, non-covalent interactions, excited states, and transition elements: two new functionals and systematic testing of four M06-class functionals and 12 other functionals. *Theor. Chem. Acc.* **2008**, *120*, 215–241.

(28) Dunning, T. H., Jr. Gaussian basis sets for use in correlated molecular calculations. I. the atoms boron through neon and hydrogen. *J. Chem. Phys.* **1989**, *90*, 1007.

(29) Kendall, R. A.; Dunning, T. H., Jr.; Harrison, R. J. Electron affinities of the first-row atoms revisited. systematic basis sets and wave functions. *J. Chem. Phys.* **1992**, *96*, 6796.

(30) Frisch, M. J.; Trucks, G. W.; Schlegel, H. B.; Scuseria, G. E.; Robb, M. A.; Cheeseman, J. R.; Scalmani, G.; Barone, V.; Mennucci, B.; Petersson, G. A.; Nakatsuji, H.; Caricato, M.; Li, X.; Hratchian, H. P.; Izmaylov, A. F.; Bloino, J.; Zheng, G.; Sonnenberg, J. L.; Hada, M.; Ehara, M.; Toyota, K.; Fukuda, R.; Hasegawa, J.; Ishida, M.; Nakajima, T.; Honda, Y.; Kitao, O.; Nakai, H.; Vreven, T.; Montgomery, J. A., Jr.; Peralta, J. E.; Ogliaro, F.; Bearpark, M.; Heyd, J. J.; Brothers, E.; Kudin, K. N.; Staroverov, V. N.; Kobayashi, R.; Normand, J.; Raghavachari, K.; Rendell, A.; Burant, J. C.; Iyengar, S. S.; Tomasi, J.; Cossi, M.; Rega, N.; Millam, J. M.; Klene, M.; Knox, J. E.; Cross, J. B.; Bakken, V.; Adamo, C.; Jaramillo, J.; Gomperts, R.; Stratmann, R. E.; Yazyev, O.; Austin, A. J.; Cammi, R.; Pomelli, C.; Ochterski, J. W.; Martin, R. L.; Morokuma, K.; Zakrzewski, V. G.; Voth, G. A.; Salvador, P.; Dannenberg, J. J.; Dapprich, S.; Daniels, A. D.; Farkas, Ö.; Foresman, J. B.; Ortiz, J. V.; Cioslowski, J.; Fox, D. J. *Gaussian 09*, revision D.01; Gaussian Inc.: Wallingford, CT, 2009.

(31) Riplinger, C.; Sandhoefer, B.; Hansen, A.; Neese, F. Natural triple excitations in local coupled cluster calculations with pair natural orbitals. *J. Chem. Phys.* **2013**, *139*, 134101.

(32) Guo, Y.; Riplinger, C.; Becker, U.; Liakos, D. G.; Minenkov, Y.; Cavallo, L.; Neese, F. Communication: An improved linear scaling perturbative triples correction for the domain based local pair-natural orbital based singles and doubles coupled cluster method [DLPNO-CCSD(T)]. *J. Chem. Phys.* **2018**, *148*, 011101.

(33) Chan, B.; Radom, L. Accurate quadruple zeta basis-set approximation for double-hybrid density functional theory with an order of magnitude reduction in computational cost. *Theor. Chem. Acc.* **2014**, *133*, 1426–1429.

(34) Liakos, D. G.; Sparta, M.; Kesharwani, M. K.; Martin, J. M. L.; Neese, F. Exploring the accuracy limits of local pair natural orbital coupled-cluster theory. *J. Chem. Theory Comput.* **2015**, *11*, 1525–1539.

(35) Neese, F. Software update: The ORCA program system, version 4.0. *WIRES: Comp. Mol. Sci.* **2018**, *8*, e1327.

(36) Zhang, S.; Krakauer, H. Quantum Monte Carlo method using phase-free random walks with Slater determinants. *Phys. Rev. Lett.* **2003**, *90*, 136401.

(37) Shee, J.; Arthur, E. J.; Zhang, S.; Reichman, D. R.; Friesner, R. A. Phaseless auxiliary-field quantum Monte Carlo on graphical processing units. *J. Chem. Theory Comput.* **2018**, *14*, 4109–4121.

(38) Shee, J.; Arthur, E. J.; Zhang, S.; Reichman, D. R.; Friesner, R. A. Singlet–triplet energy gaps of organic biradicals and polyacenes with auxiliary-field quantum Monte Carlo. *J. Chem. Theory Comput.* **2019**, *15*, 4924–4932.

(39) Shee, J.; Rudshteyn, B.; Arthur, E. J.; Zhang, S.; Reichman, D. R.; Friesner, R. A. On achieving high accuracy in quantum chemical calculations of 3d transition metal-containing systems: A comparison of auxiliary-field quantum Monte Carlo with coupled cluster, density functional theory, and experiment for diatomic molecules. *J. Chem. Theory Comput.* **2019**, *15*, 2346–2358.

(40) Goddard, W. A., III; Dunning, T. H., Jr.; Hunt, W. J.; Hay, P. J. Generalized valence bond description of bonding in low-lying states of molecules. *Acc. Chem. Res.* **1973**, *6*, 368–376.

(41) Laidig, W. D.; Schaefer, H. F., III Large multiconfiguration self-consistent-field wave functions for the ozone molecule. *J. Chem. Phys.* **1981**, *74*, 3411.

(42) Kucharski, S. A.; Bartlett, R. J. An efficient way to include connected quadruple contributions into the coupled cluster method. *J. Chem. Phys.* **1998**, *108*, 9221.

(43) Purwanto, W.; Krakauer, H.; Virgus, Y.; Zhang, S. Assessing weak hydrogen binding on Ca^+ centers: an accurate many-body study with large basis sets. *J. Chem. Phys.* **2011**, *135*, 164105.

(44) Perdew, J. P.; Wang, Y. Accurate and simple analytic representation of the electron-gas correlation energy. *Phys. Rev. B: Condens. Matter Mater. Phys.* **1992**, *45*, 13244.

(45) Perdew, J. P.; Burke, K.; Ernzerhof, M. Generalized gradient approximation made simple. *Phys. Rev. Lett.* **1996**, *77*, 3865.

(46) Grimme, S. Accurate description of van der Waals complexes by density functional theory including empirical corrections. *J. Comput. Chem.* **2004**, *25*, 1463–1473.

(47) Grimme, S. Semiempirical GGA-type density functional constructed with a long-range dispersion correction. *J. Comput. Chem.* **2006**, *27*, 1787–1799.

(48) VandeVondele, J.; Krack, M.; Mohamed, F.; Parrinello, M.; Chassaing, T.; Hutter, J. Quickstep: fast and accurate density functional calculations using a mixed Gaussian and plane waves approach. *Comput. Phys. Commun.* **2005**, *167*, 103–128.

(49) Donaldson, D. J.; Vaida, V. The influence of organic films at the air-aqueous boundary on atmospheric processes. *Chem. Rev.* **2006**, *106*, 1445–1461.

(50) Ravishankara, A. R. Heterogeneous and multiphase chemistry in the troposphere. *Science* **1997**, *276*, 1058–1065.

(51) Zhong, J.; Kumar, M.; Zeng, X. C.; Francisco, J. S. Insight into chemistry on cloud/aerosol water surfaces. *Acc. Chem. Res.* **2018**, *51*, 1229–1237.

(52) Goedecker, S.; Teter, M.; Hutter, J. Separable dual-space Gaussian pseudopotentials. *Phys. Rev. B: Condens. Matter Mater. Phys.* **1996**, *54*, 1703.

(53) Hartwigsen, C.; Goedecker, S.; Hutter, J.; Hartwigsen, C.; Goedecker, S.; Hutter, J. Relativistic separable dual-space Gaussian pseudopotentials from H to Rn. *Phys. Rev. B: Condens. Matter Mater. Phys.* **1998**, *58*, 3641.

(54) Criegee, R. Mechanism of ozonolysis. *Angew. Chem., Int. Ed. Engl.* **1975**, *14*, 745–752.

(55) Razumovskii, S. D.; Zaikov, G. E. *Ozone and Its Reactions with Organic Compounds (Studies in Organic Chemistry)*; Elsevier Science Ltd: New York, 1984.

(56) Razumovskii, S. D.; Gennadii, E. Z. Kinetics and mechanism of the reaction of ozone with double bonds. *Russ. Chem. Rev.* **1980**, *49*, 1163–1180.

(57) Atkinson, R.; Carter, W. P. L. Kinetics and mechanisms of the gas-phase reactions of ozone with organic compounds under atmospheric conditions. *Chem. Rev.* **1984**, *84*, 437–470.

(58) DeMore, W. B. Arrhenius constants for the reactions of ozone with ethylene and acetylene. *Int. J. Chem. Kinet.* **1969**, *1*, 209–220.

(59) Chan, W.-T.; Hamilton, I. P. Mechanisms for the ozonolysis of ethene and propene: Reliability of quantum chemical predictions. *J. Chem. Phys.* **2003**, *118*, 1688–1701.

(60) Krisyuk, B.; Maiorov, A. Competition between the concerted and nonconcerted addition of ozone to a double bond. *Russ. J. Phys. Chem. B* **2011**, *5*, 790–796.

(61) Krisyuk, B. E.; Popov, A. A. Addition of Ozone to Multiple Bonds. Competition of the Reaction Pathways. In *Chemical and Biochemical Physics, Kinetics and Thermodynamics: New Perspectives*; Stott, P. E., Zaikov, G. E., Kablov, V. F., Eds.; Nova Science Publishers Inc.: Hauppauge, NY, 2008.

(62) Deng, J.; Chen, J.; Geng, C.; Liu, H.; Wang, W.; Bai, Z.; Xu, Y.-S. The overall reaction process of ozone with methacrolein and isoprene in the condensed phase. *J. Phys. Chem. A* **2012**, *116*, 1710–1716.